Origin of Stratification in Creaming Emulsions

Daniel M. Mueth, John C. Crocker, Sergei E. Esipov, and David G. Grier
The James Franck Institute and Department of Physics, The University of Chicago, 5640 S. Ellis Ave., Chicago, Illinois 60637
(Received 10 January 1996)

Colloidal suspensions aging under gravity have long been known to spontaneously separate into layers. We demonstrate through flow visualization experiments that a lateral temperature gradient as small as 10 mK/cm can be responsible for such stratification and that strata correspond to a stack of convection rolls. A linear stability analysis suggests that the onset of stratification results from a convective instability peculiar to fluids with inhomogeneous mass densities subjected to lateral thermal gradients. [S0031-9007(96)00672-2]

PACS numbers: 82.70.Kj, 47.20.Bp, 47.55.Hd

Initially homogeneous colloidal suspensions often stratify as they settle under gravity with a stratified suspension's density changing abruptly at sharp interfaces between horizontal layers. The discrete layers can be observed easily using the light scattered by the colloidal particles. Photographs in Fig. 1 show six stages in the spontaneous stratification of a column of decane emulsion. Such layer formation already was well known by 1884 when Brewer [1] described his observations on sedimenting clay suspensions. Subsequent reports over the past century have described stratification in monodisperse [2–4] and polydisperse [1,5–9] suspensions of spherical and irregularly shaped [8,9] colloidal particles. Stratification has been seen for bouyant particles which cream to the top of their suspension as well as for dense particles which settle to the bottom.

Several mechanisms have been proposed to explain these observations, including spinodal decomposition in the fluid ensemble of particles [2], the formation of vertical streaming flows [10], and the generation of a sequence of Burgers shocks [11]. We describe experiments on creaming emulsions which demonstrate that each layer in a stratified suspension is a discrete convention roll and that the stack of co-rotating convection rolls is driven by a small horizontal thermal gradient. We suggest that these rolls are created by a convective instability due to a coupling between a vertical gradient in the concentration of suspended particles and the horizontal thermal gradient.

The decane-in-water emulsions used in this study were prepared by inversion emulsification using Pluronic F88 surfactant to stabilize the resulting decane droplets against recombination. The droplet diameters were determined by digital video microscopy to follow a log-normal distribution peaked at 0.6 μm with most droplet diameters falling between 0.3 and 1.2 μm. Repeated observations on well-mixed samples suggest that the emulsion is stable against aggregation over the duration of these experiments.

The emulsions were diluted with deionized water to decane volume fractions, ϕ, ranging from 10^{-3} to 10^{-4} and were placed in glass tubes 30 cm tall with inner diameters ranging between 8 and 22 mm. As suggested by the literature, we strove to isolate the tubes from thermal gradients by placing them in a dark, vacant, and windowless room. Under these conditions, we would expect the decane droplets to rise in the column with the creaming velocity

$$\vec{v} = \frac{2}{9}\,\frac{a^2\Delta\rho}{\nu}\,\vec{g}\,, \tag{1}$$

where a is the radius of the droplet, $\Delta\rho$ is the density mismatch between the sphere and the fluid ($\rho_{\text{decane}} - \rho_{\text{water}} = -0.27\ \text{g/cm}^3$), ν is the viscosity of the fluid (0.01 P for water), and $\vec{g}$ is the acceleration due to

FIG. 1. Images of a 12 mm inner diameter vertical tube of emulsion evolving over time. Visible intensity steps in the rightmost photographs indicate steps in decane droplet concentration, with brighter regions having higher concentration. From left to right, photos were taken after 0, 51, 73, 100, 137, and 175 h of creaming.

 0031-9007/96/77(3)/578(4)$10.00

gravity. For a 0.6 μm diameter decane droplet in water, the creaming rate is 0.26 μm/sec or, equivalently, 2.2 cm/day.

The counterflow of water around an ensemble of creaming particles reduces the rate at which they rise. In a dilute system, the reduction depends linearly on the droplet concentration [12,13] and causes concentration gradients to self-sharpen [14] in a manner described by a Burgers equation [15]. Such gradients form as an initially homogeneous emulsion creams, leaving depleted solvent at the bottom of the column and forming concentrated cream at the top. Their sharpness is moderated by diffusion and differential creaming [16].

We monitored the evolution of the decane volume fraction in our columns by photographing them at roughly 12 h intervals. Photographs such as those in Fig. 1 were taken against a dark background with side illumination from a fluorescent light box. The results of our observations qualitatively resemble those of earlier reports. Their most general features can be summarized in five points. (1) Several 1–2 mm tall strata suddenly appear in the concentration gradient near the bottom of the column after two or three days of creaming. These then rise through the column while spreading out, as shown in Fig. 2. (2) The optical density within each layer appears to be uniform, suggesting that the emulsion in each layer is homogeneous. (3) The interfaces between layers move at roughly the creaming velocity of the droplets. (4) The interfaces between layers can be disrupted by a small heat source such as a flashlight or a nearby observer, and yet (5) thermally shielding a suspension by placing it in a stirred water bath or in an insulated enclosure prevents stratification altogether.

Since observations (4) and (5) suggested sensitivity to thermal gradients, we placed tubes inside an insulated enclosure with a heat source on one side to apply a small controlled thermal gradient. These tubes reproducibly formed multiple layers when the thermal gradient was applied, and not otherwise. Removing the gradient caused the layers in a stratified column to blur to invisibility within a few hours. Reapplying the gradient caused strata to reappear in less than a half hour. The temperature drop across the tube was measured using a pair of low mass thermocouples and a low drift differential amplifier to be 1 $\pm$ 2 mK with the heat source off and 10 $\pm$ 2 mK with it on. A thermal gradient of this magnitude could have arisen in the earlier experiments if the temperature of opposite walls in the room differed by about 1 K.

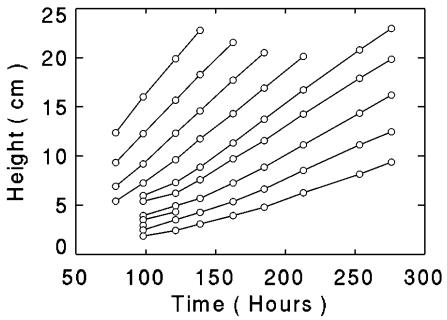

FIG. 2. Positions of the strata boundaries for the tube in Fig. 1 as a function of creaming time.

Even such small lateral thermal gradients can drive convection in an incompressible homogeneous fluid. Hydrostatic equilibrium requires the fluid's mass density, ρ_0, to be a function only of the height [17]. A fluid whose density depends only on temperature therefore must convect in the presence of a horizontal thermal gradient. The flow profile for a homogeneous fluid contained in a vertical cylinder of diameter d and subjected to a uniform horizontal temperature gradient $\Delta T/d$ directed along the in-plane angle $\psi = 0$ is

$$v_z = -\frac{\beta_g \Delta T}{8\nu d}\left(r^3 - \frac{1}{4}d^2 r\right)\cos\psi\,, \qquad (2)$$

where β is the thermal expansion coefficient for the fluid. Substituting typical values for our experiment ($\beta = 2.2 \times 10^{-4}\ \mathrm{K}^{-1}$, $\Delta T = 10$ mK, $d = 1$ cm), suggests a convective flow of roughly 10 μm/sec, which is more than an order of magnitude greater than the creaming velocity.

A simple flow visualization experiment demonstrates a strong correlation between convection and stratification. Small ribbons of paper soaked with nigrosin dye and weighted at one end with epoxy were dropped down the center line of a stratified emulsion column as shown in Fig. 3. Distortions of the dye trail map out lateral fluid flow in the column. High shear regions were observed reproducibly at the interfaces between strata. This combined with the measured thermal gradient strongly suggests that each layer is a single convection roll.

This scenario accounts for several of our qualitative observations. First, since the convection velocity is considerably larger than the creaming velocity of the particle, flow tends to homogenize the contents of each roll. Second, since convective flow must vanish at the interface between adjacent rolls, the emulsion at the interface, and therefore the interface itself, rises at the creaming velocity. In our polydisperse suspensions, larger more buoyant droplets rise fastest and populate the upper strata whose interfaces correspondingly rise faster than those between lower strata. Such spreading is evident in Fig. 2. Finally, the range of temperature gradients over which stratifying convection should occur is limited by competition among the forces acting within the system. The temperature gradient should be large enough that convection dominates sedimentation:

$$\Delta T > \Delta T_{\min} \approx \frac{30}{\beta}\frac{|\Delta\rho|}{\rho}\left(\frac{a}{d}\right)^2. \qquad (3)$$

$\Delta T_{\min}$ for our system is less than 100 μK. If the temperature gradient is too large, however, the hydrodynamic

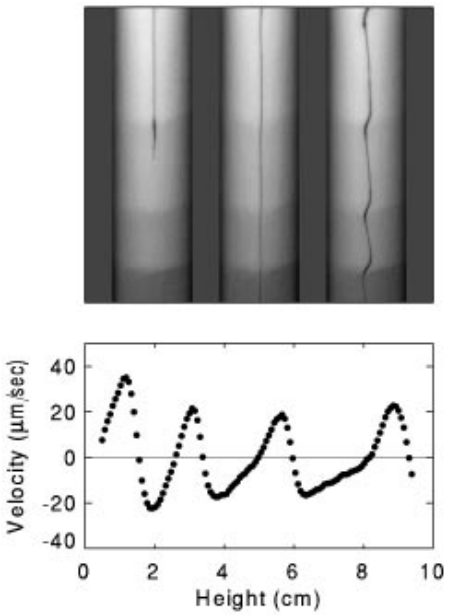

FIG. 3. Direct visualization of convective flow in a stratified suspension. Top: Three photographs following the time evolution of a line of dye in a 22 mm inner diameter tube of stratified emulsion. A small heat source, located to the right in the plane of the photograph, was used to set up a constant 10 mK temperature difference across the tube. The leftmost photograph shows a weighted projectile impregnated with nigrosin dye falling down the centerline of the tube, leaving a dye stream in its wake. The other two photographs show the system 5 and 35 sec later. Deformation of the dye line clearly indicates small fluid flows in the suspension with high gradients precisely at the boundaries between the strata, visible as the faint banding in the tube. Simultaneous observations from the side showed no deformation out of the plane of the photograph. Bottom: The horizontal flow velocity along the tube's center line as measured from the photographs above.

torque exerted by counterpropagating flows meeting at an interface exceeds the gravitational restoring torque and destabilizes the interface. Thus we require

$$\Delta T < \Delta T_{\max} \approx \frac{\nu}{\beta}\left(\frac{|\Delta\rho\Delta\phi|}{\rho g d^3}\right)^{1/2}, \tag{4}$$

where $\Delta\phi$ is the difference in droplet volume fraction between adjacent rolls. $\Delta T_{\max}$ for our system is roughly 50 mK, and could easily be generated by a flashlight or the body heat of a nearby observer.

As early as 1923, Mendenhall and Mason [6] suggested that layering might be the result of convection driven by a lateral thermal gradient, and visualized convection rolls by adding dye. Unfortunately, they did not estimate the magnitude of the thermal gradient present in their system, nor did they publish photographs of their visualization experiments. Their observations were dismissed at that time as being irreproducible [18]. More recently, Siano [2] discouraged consideration of convective stratification, arguing that flows such as that described by Eq. (2) result in system-spanning convection cells rather than stacks of small rolls. This analysis, however, applies only to homogeneous fluids. By considering the dependence of a suspension's mass density on the volume fraction of suspended material, we can explain the onset of stratified convection.

The Navier-Stokes equations for an incompressible inhomogeneous suspension are

$$\frac{\partial\vec{v}}{\partial t} = -\frac{1}{\rho_0}\vec{\nabla}p + \left[\frac{\Delta\rho}{\rho_0}\phi + \beta T\right]\vec{g} + \nu\nabla^2\vec{v}, \tag{5a}$$

$$D\nabla^2\phi = \frac{\partial\phi}{\partial t} + \vec{v}\cdot\vec{\nabla}\phi, \tag{5b}$$

and

$$\vec{\nabla}\cdot\vec{v} = 0, \tag{5c}$$

where p is the pressure, ρ_0 is the fluid's mean density, $\vec{v}$ is the velocity, ϕ is the volume fraction of the suspended droplets, D is their diffusion coefficient, and T is the temperature. For slow flow, we can neglect the effect of convective heat transport and take T to be a static field.

The fluid remains in hydrostatic equilibrium provided its mass density, proportional to the term in square brackets in Eq. (5a), depends only on height, z. To compensate a lateral temperature gradient, the concentration of suspended material must satisfy

$$\frac{\partial\phi_0}{\partial x} = -\beta\frac{\rho_0}{\Delta\rho}\frac{\partial T}{\partial x}. \tag{6}$$

Equation (6) is equivalent to requiring the concentration gradient $\vec{\nabla}\phi$ to make an angle

$$\alpha \equiv \tan^{-1}\left[\beta\frac{\rho_0}{\Delta\rho}\frac{\partial T}{\partial x}\left(\frac{\partial\phi_0}{\partial z}\right)^{-1}\right] \tag{7}$$

with the z axis. For our system, $\alpha \ll 1$.

A small perturbation

$$\phi = \phi_0(1 + \delta e^{i\vec{k}\cdot\vec{r} - i\omega t}) \tag{8}$$

away from the equilibrium state generates a proportionately large convective flow $\vec{v}$ transverse to $\vec{k}$. Substituting ϕ and $\vec{v}$ into Eqs. (5) yields the dispersion relation

$$(\omega + iDk^2)(\omega + i\nu k^2) = -g\frac{\Delta\rho}{\rho_0}\frac{\partial\phi_0}{\partial z}\left(\sin^2\theta - \frac{1}{2}\sin\alpha\,\sin 2\theta\right), \tag{9}$$

where θ is the angle between the wave vector $\vec{k}$ and the vertical axis. The vertical gradient in the mass density, $\Delta\rho\,\partial\phi_0/\partial z$, is strictly negative in a sedimenting (or creaming) suspension.

Horizontally directed wave vectors ($\theta = \pi/2$) reduce Eq. (9) to a form describing damped gravity waves with a characteristic frequency $\omega_0 = \sqrt{|g(\Delta\rho/\rho_0)\partial\phi_0/\partial z|}$. This damped oscillatory behavior suggests that the system

tends toward the equilibrium state described by Eq. (6), and that this is an appropriate starting point for a linear stability analysis.

Perturbations for which the right-hand side of Eq. (9) is negative are unstable and grow exponentially rapidly. The fastest growing modes, and thus those most likely to be manifested, have wave vectors directed almost vertically with $\theta \approx \alpha/2$ in the long-wavelength limit. Since such wave vectors describe horizontal flows, it is not unreasonable to suggest that each spatial period of the fastest growing mode eventually develops into one convection roll in the stratified column.

The wavelength of the maximally unstable mode depends on the details of the boundary conditions and so does not emerge from this analysis. However, the term proportional to k^4 on the left-hand side of Eq. (9) stabilizes the system against short-wavelength perturbations and leads to a prediction for the marginally stable wavelength

$$\lambda_0 = \left[64\pi^4 \frac{D\nu}{\beta^2 g} \frac{d^2}{\Delta T^2} \left(-\frac{\Delta\rho}{\rho_0} \frac{\partial \phi_0}{\partial z} \right) \right]^{1/4}, \qquad (10)$$

which serves as a rough estimate for the observed wavelength. Estimating $\partial\phi_0/\partial z = 10^{-4}$ cm^{-1} from the region where strata first appear in Fig. 1 yields $\lambda_0 \approx$ 2 mm, in very good agreement with the observed initial interfacial separation.

Including no-flow source-free boundary conditions in the above calculation indicates that there are no unstable modes for vertical linear concentration gradients of extent less than a threshold, $L(d)$. The minimum threshold, $L \approx 3$ mm, is achieved in wide columns. This analysis suggests that the delay for the onset of stratification is simply the time required for differential creaming and diffusion to create a weak volume fraction gradient of sufficient spatial extent. Deliberately creating a vertical composition gradient induces immediate stratification [2].

The above analysis does not depend on microscopic details of the fluid. Similar stratification should occur for monodisperse suspensions and simple solutions, provided the necessary density and thermal gradients are present. Since the diffusion coefficients, D, for dissolved molecules are so much larger than those for colloidal particles, the length and time scales for solutions could be considerably larger than for the experiments we describe. For example, we speculate that such convective instabilities play a role in the formation of the thermohaline staircase profiles often observed in oceans [19].

This Letter has not addressed interactions and material transfer between adjacent convection rolls. These effects could explain the occasionally observed coalescence and division of layers, and merit further study.

While convective stratification provides a reasonable explanation for the experiments we describe, Burgers dynamics can produce qualitatively similar phenomena in the absence of convection. Sequences of Burgers shocks have been predicted to form in nonconvecting suspensions with density gradients imposed either by initial conditions [11] or by differential sedimentation [16]. Still, since the preponderance of experiments reported in the literature (for example, [1–3,5–9]) did not employ stringent thermal isolation, they most likely operated under conditions which favor convective stratification.

It is a pleasure to acknowledge enlightening conversations with Leo Kadanoff, Todd Dupont, Anette Hosoi, Robert Gomer, and David Kielpinski. This work was supported in part by the MRSEC Program of the National Science Foundation under Award No. DMR-9400379, in part by the National Science Foundation under Grant No. DMR-9320378, and in part by the donors of the American Chemical Society through the Petroleum Research Fund.

[1] W. H. Brewer, Clays Clay Miner. **13**, 395 (1884).
[2] D. Siano, J. Colloid Interface Sci. **68**, 111 (1979).
[3] Y. S. Papir and I. M. Krieger, J. Colloid Interface Sci. **34**, 126 (1970).
[4] M. C. Anselmet, R. Anthore, X. Auvray, C. Pepitas, and R. Blanc, C. R. Acad. Sci. Paris **300**, 933 (1985).
[5] C. Barus, Bull. U.S. Geol. Surv. **5**, 515 (1886).
[6] C. E. Mendenhall and M. Mason, Proc. Natl. Acad. Sci. **9**, 199 (1923).
[7] C. G. T. Morison, Proc. R. Soc. London Ser. A **108**, 280 (1925).
[8] T. J. Tobias and A. P. Ruotsala, Clays Clay Miner. **13**, 395 (1966).
[9] S. R. Merchant and E. A. Rosauer, Clays Clay Miner. **17**, 289 (1969).
[10] W. H. Bradley, Science **150**, 1423 (1965).
[11] W. van Saarloos and D. A. Huse, Europhys. Lett. **11**, 107 (1990).
[12] A. Einstein, Ann. Phys. **34**, 591 (1911).
[13] G. K. Batchelor, J. Fluid Mech. **52**, 245 (1972).
[14] G. J. Kynch, Trans. Faraday Soc. **48**, 166 (1952).
[15] G. O. Barker and M. J. Grimson, J. Phys. A **20**, 305 (1987).
[16] S. E. Esipov, Phys. Rev. E **52**, 3711 (1995).
[17] L. D. Landau and E. M. Lifshitz, *Fluid Mechanics* (Pergamon, Oxford, 1984), pp. 6–10.
[18] P. G. Nutting, J. Wash. Acad. Sci. **19**, 402 (1929).
[19] R. W. Schmitt, Ann. Rev. Fluid Mech. **26**, 255 (1994).